A R C H I V E S O F M E T A L L U R G Y A N D M A T E R I A L S
Volume 60 2015 Issue 4
DOI: 10.1515/amm-2015-0426

K. ŻABA*,#, M. NOWOSIELSKI*, S. PUCHLERSKA*, M. KWIATKOWSKI*, P. KITA*, M. GŁODZIK*, K. KORFANTY*, D. POCIECHA*, T. PIEJA**

INVESTIGATION OF THE MECHANICAL PROPERTIES AND MICROSTRUCTURE OF NICKEL SUPERALLOYS PROCESSED IN SHEAR FORMING

IDENTYFIKACJA WŁAŚCIWOŚCI MECHANICZNYCH ORAZ MIKROSTRUKTURY SUPERSTOPÓW NIKLU PRZETWARZANYCH W PROCESIE KSZTAŁTOWANIA OBROTOWEGO

The paper presents the research results of the mechanical properties and microstructure of the material in initial state and parts made from nickel superalloy Inconel®718 in the rotary forming process with laser heating. In the first step was carried out basic research of chemical composition, mechanical properties, hardness and microstructure of sheet in initial state. Then from the metal sheet, in industrial conditions, was made axisymmetric parts in the flow and shear forming with laser heating. Parts were subjected to detailed studies focused on the analysis of changes in the mechanical properties and microstructure in the relation to the material in initial state. The analysis was based on the tests results of strength and plastic properties, hardness, microstructural observations and X-ray microanalysis in the areas where defects appear and beyond. The results are presented in the form of tables, charts, and photographs of the microstructure.

W publikacji przedstawiono wyniki badań właściwości mechanicznych oraz mikrostruktury materiału wsadowego i wyrobów wykonanych z superstopu niklu Inconel®718 w procesie kształtowania obrotowego z nagrzewaniem laserowym. W pierwszym etapie zrealizowano podstawowe badania składu chemicznego, właściwości mechanicznych, twardości oraz mikrostruktury blachy wsadowej. Następnie z blachy, w warunkach przemysłowych, wykonano wyroby osiowosymetryczne w procesie kształtowania obrotowego metodą flow i shear formingu z nagrzewaniem laserowym. Wyroby poddano szczegółowym badaniom ukierunkowanym na analizę zmian właściwości mechanicznych oraz mikrostruktury w stosunku do materiału wsadowego. Podstawą analizy były wyniki z testów właściwości wytrzymałościowych i plastycznych, twardości oraz obserwacji mikrostrukturalnych i mikroanalizy rentgenowskiej w obszarach zarówno z wadami, jak i poza nimi. Wyniki przedstawiono w postaci tablic, wykresów oraz fotografii mikrostruktury.

1. Introduction

Heat resistant nickel superalloys Inconel type are widely used materials in the aerospace industry, primarily in the manufacture of aircraft engine components [1]. Their use in this demanding industrial field, determine the unique combination of fatigue strength at high temperature, creep strength and oxidation resistance [2]. Heat-resistant matrix of these alloys is a combination of components Ni-Cr-Co-Mo with additions of Ti and Al in appropriate proportions. These alloying elements precipitated in the form of different phases may cause a decrease of alloys ductility in the range of 590-980°C [3]. The complex structure of the nickel superalloy Inconel type can be modified as a result of even a small change in the chemical composition, changes in heat treatment parameters, or parameters of processing. The relationship between the structure of the nickel superalloys and their finally properties are well understood in the range of temperature 650-1100°C [4-5].

Inconel alloys are designed i.e. for the production of thin-walled, axisymmetric shells elements of jet engine combustion chamber. One of the producing technique is a rotary forming process using spinning, flow and shear forming methods [6-12]. Change of the shape and dimensions of the batch disc carries out with a tools in the form of rolls and a template, by two operations: a spinning – with no change or minimal change in wall thickness, and flow forming – with a controlled change in wall thickness. The process is carried out in several stages with a small degree of deformation in each of them. Due to the specific properties of Inconel alloys, which are a high deformation resistance, caused by a high intensity of strengthening and high temperature of recrystallization, design forming processes for these alloys is a complex task. There are being attempts of plastic forming at elevated temperatures [13-14]. Both in the process carried out cold, as well as elevated temperature, there are a number of faults in the form of free and cylindrical part waves, peripheral and radial cracks, resulting

* AGH UNIVERSITY OF SCIENCE AND TECHNOLOGY, FACULTY OF NON-FERROUS METALS ,AL. A. MICKIEWICZA 30, 30-059 KRAKOW, POLAND
** PROTT AND WHITNEY, RZESZÓW, POLAND
# Corresponding author: krzyzaba@agh.edu.pl

both from the essence of the process, so flow mechanics, as well from the state of the deformed material microstructure.

The paper presents results of research on the analysis of the mechanical properties and microstructure of the material in initial state and products made of nickel superalloy Inconel®718 in the rotary forming process with laser heating.

2. Experimental procedure

For tests were chosen sheets from a commercial Inconel®718 alloy with a thickness of 3 mm. In the first of the study was made the analysis of the chemical composition in the initial state by use of an ICP method (Inductively Coupled Plasma). The study was carried out using a spectrophotometer (ICP-OES) Plasma 40 Perkin Elmer with inductively coupled plasma.

Next was performed the tests of mechanical properties of the material in initial state, on samples cut from the sheet at an angle 0, 45 and 90° relative to the rolling direction. For this purpose, the uniaxial tensile test according to the standard [14]. The study was carried out using a static machine Zwick/Roell Z050. The machine was operated and controlled using the program testXpert® II. This program was also used to collect data from the tensile test. Additionally was carried out Rockwell hardness testing of material in initial state according to [16].

Study of the microstructure was carried out on samples cut from the sheets, which were prepared using a device ROTOPOL 11, Struers. The samples was poured in EPOFIX Struers resin and then polished using sandpaper with gradation of 220-1100 mm and polished on polishing discs, using diamond suspensions with gradation of 15, 9, 6, 3, 1 mm. Observations of the structure was performed using a scanning electron microscope Hitachi Su-70. The structure was analyzing in the perpendicular and parallel direction relative to the rolling direction. In the study was also carried WDS analysis using a scanning electron microscope Hitachi Su-70.

The second stage, carried out in industrial conditions were experimental studies involving the manufacture of axisymmetric metal products, in the process of spinning, flow and shear forming with a local laser heating. Schematic configuration is shown in fig. 1.

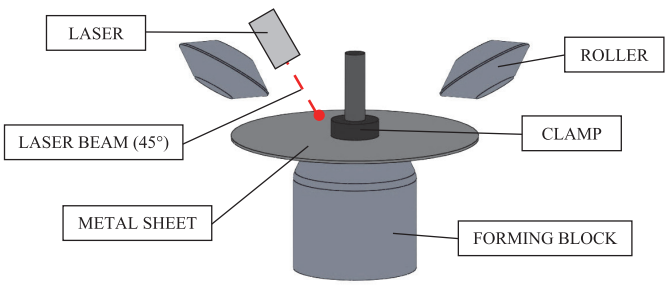

Fig. 1. Schematic configuration of rotary forming process with a local laser heating

Feedstock to the process was a sheet of Inconel®718 material in the form of disc with a thickness of 3 mm and a diameter of 250 mm. For the study used the commercial, industrial Leifeld device. Fig. 2a shows a shell element made by rotary forming with the marked areas, from which test samples were cut. Fig. 2b shows a fragment of the final product.

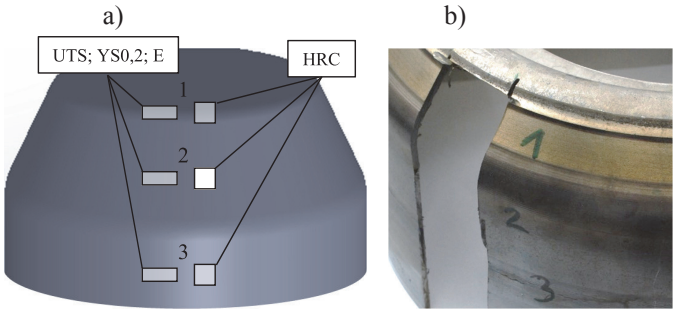

Fig. 2. Scheme of the shell element made by rotary forming process with marked areas, from which tests samples were cut (a) and a fragment of the final product (b)

The angle of the laser beam was 45°, the temperature in the center of laser impact was approx. 840°C, and the heating time was 4 minutes. The rotational speed of the forming roll was 250 RPM. The radius of the forming roll was equal to R=20 mm. The final shape of the product having a thickness of 2,1 mm was obtained in 27 passes. From the product, according to the scheme in fig. 2, the test samples were cut for testing mechanical properties and microstructural observations. The study was conducted in accordance with the methodology adopted for the material in initial state. In addition, were made EDS mapping using a scanning electron microscope Hitachi Su-70, for the analysis of the elements distribution in the test areas.

The results of the study are presented in the form of tables, charts and microscopic observation.

3. Results

3.1. The test results of Inconel®718 sheets in initial conditions

The results of ICP analysis of the chemical composition of the Inconel®718 sheet in initial state are shown in table 1.

As expected, the dominant component of the alloy is nickel content of approx. 52%. The content of iron and chromium is approx. 20-21%, and molybdenum approx. 3%. Additional ingredients comprising the alloy are titanium, aluminum, lead and vanadium.

TABLE 1

The chemical composition of Inconel®718 [wt. %]

Ni	Fe	Cr	Mo	Ti	Al	Pb	Si	V	Cu	Mn
52,07	21,03	20,29	3,38	0,99	0,58	0,56	0,18	0,09	0,09	0,06

3.1.1 The results of mechanical properties

The mechanical characteristics of the sheet was determinated based on the static tensile test. The yield strength $YS_{0,2}$; tensile strength UTS and elongation A was determined. The averaged values in the plane of the sheet are rounded to 1MPa, respectively, in the case of mechanical properties and up to 1% for plastic properties. The results of the strength properties of the sheet shown in figs. 3-4.

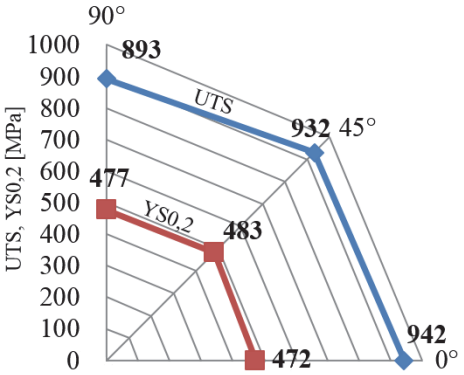

Fig. 3. The results of mechanical properties of Inconel®718 sheet

The strength properties of the sheet slightly dependent on the sampling relative to the rolling direction. Tensile strength UTS in the direction parallel to the rolling direction reaches UTS_0= 942MPa, decreases for sample at 45° relative to the rolling direction to the $UTS_{45°}$= 932MPa, and for samples taken at 90° relative to the rolling direction reaches the lowest value $UTS_{90°}$=893MPa. The yield strength $YS_{0,2}$ reaches the highest value for the samples collected at 45° to the rolling direction $YS_{0,2\text{-}45°}$=483MPa, an intermediate value for samples collected at 90° to the rolling direction $YS_{0,2\text{-}90°}$= 477MPa and the lowest value for the sample cut parallel to the rolling direction $YS_{0,2}$=472MPa.

The results of the plastic properties of the sheet is shown in fig. 4.

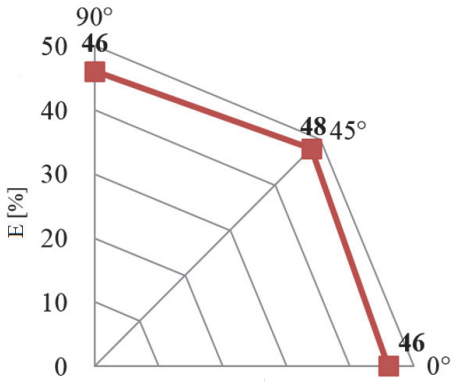

Fig. 4. The results of plastic properties of Inconel®718 sheet

Plastic properties evaluated by elongation A are not dependent on the sampling direction in relation to the rolling direction of the sheet. Elongation for samples taken parallel to the rolling direction is E_0=46%, increases for samples taken at an angle of 45° to the rolling direction to the $E_{45°}$=48%, and then decreases for samples taken at 90° to the value $E_{90°}$=46%.

The test results of strength and plastic properties suggest no anisotropy influence of Inconel®718 sheet in initial conditions.

Noteworthy is advantageous from the point of view of test sheet susceptibility for stamping, the low value of $YS_{0,2}$/UTS=0,5-0,53 regardless of the sampling direction, providing a high "reserve strength" of the material.

The average Rockwell hardness of the sheet in initial state is 17,2 HRC.

3.1.1 The results of microstructural observations

Fig. 5-6 shows the structure observation of material in the initial state, made with a scanning electron microscope, cut in a perpendicular and parallel direction relative to the rolling direction.

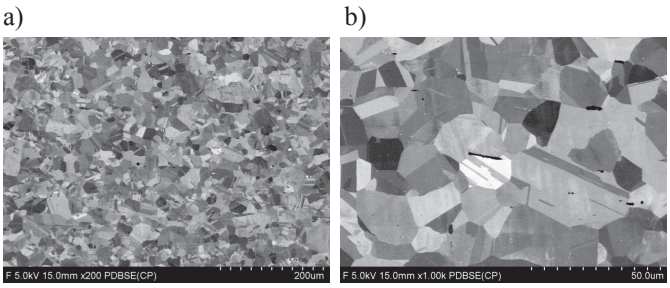

Fig. 5. The microstructure of the Inconel®718 sheet in initial conditions in perpendicular direction relative to the rolling direction a) ×200, b) ×1,00k

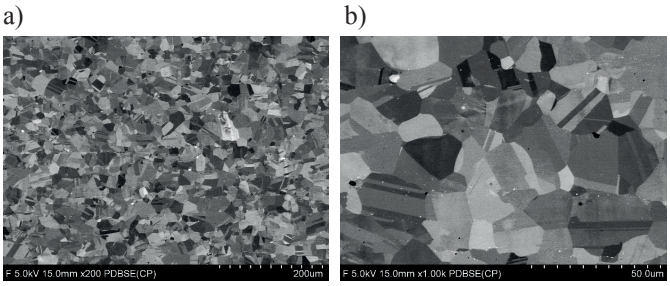

Fig. 6. The microstructure of the Inconel®718 sheet in initial conditions in parallel direction relative to the rolling direction a) ×200, b) ×1,00k

Observations suggest recrystallized structure of Inconel®718 sheet after annealing. Grains have clear boundaries, along which are visible precipitations. In the case of Inconel®718 alloy are mainly of chromium, niobium, titanium and molybdenum carbides [17]. This type of large, porous precipitation influence the nucleation of cracks. Small white points are precipitation of heavy elements, usually molybdenum compounds, distributed mainly at the grain boundaries [17]. Some of these precipitates are too small to be able to accurately analyze their chemical composition, although conclusions on their chemical composition, can be drawn on the basis of the SEM characteristics studies in BSE contrast.

Fig. 7-8 shows the structure of the surface layer of the Inconel®718 sheet in initial state.

a) b)

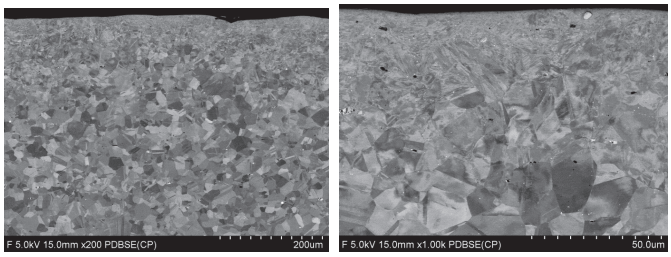

Fig. 7. The structure of the surface layer of the Inconel®718 sheet in initial state in a perpendicular direction to the rolling direction,
a) the recrystallized inner layer with surface layer, ×200,
b) the deformed surface layer of the sheet, ×1,00k

a) b)

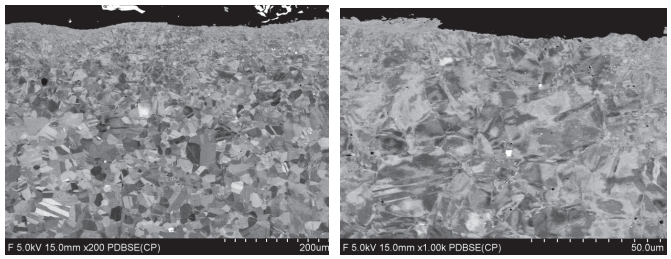

Fig. 8. The structure of the surface layer of the Inconel®718 sheet in initial state in a parallel direction to the rolling direction,
a) the recrystallized inner layer with surface layer, ×200,
b) the deformed surface layer of the sheet, ×1,00k

A characteristic feature of the surface layer is its fine-grained structure. This is probably the smoothing effect, which the surface sheet is rolling after recrystallization annealing. The thickness of the layer is approx. 40μm.

To determine the chemical composition of the matrix and precipitations (fig. 9) was carried out WDS X-ray microanalysis. The results are shown in fig. 10 and table 2.

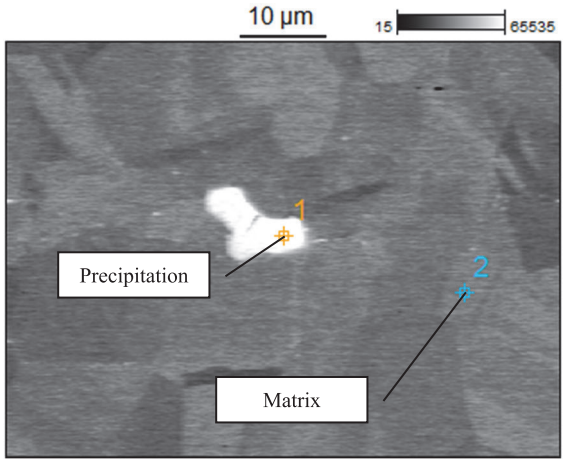

Fig.9. The microstructure of the Inconel®718 sheet in initial state,
1 – precipitation,
2 – matrix

a)

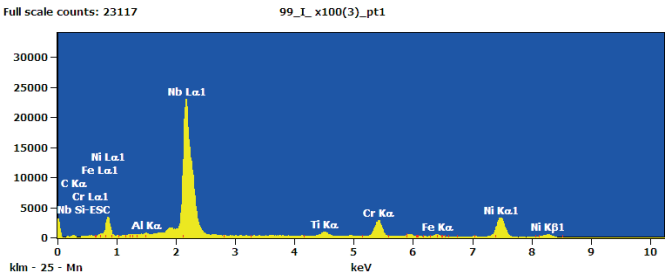

b)

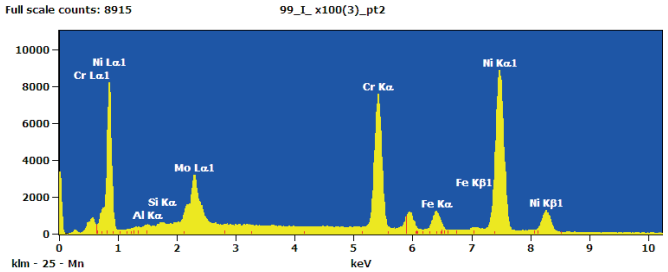

Fig.10. Diffractograms of Inconel®718 sheet in initial state,
a) precipitation,
b) matrix

The white area in fig. 9 this is precipitation, mainly containing in composition niobium and carbon, which confirms the quantitative analysis shown in fig. 10 and table 2. Precipitation is probably niobium carbide, which is confirmed by the results of published work [17-18]. Matrix (fig. 9) consists mainly of nickel and chromium (fig. 10, table 2) forming alloyed austenite.

3.2. The results of Inconel®718 sheet after rotary forming process with laser heating.

3.2.1 The results of mechanical properties

The mechanical characteristics of the material samples from three areas of the product (fig. 2a), obtained after rotary forming with laser heating, determined based on the static tensile test, as for the sheet in initial state. The results of tensile properties of the material after deformation is shown in fig. 11.

TABLE 2

The chemical composition of the precipitation and matrix of the Inconel®718 sheet

Component [wt. %]	C	Al	Si	Ti	Cr	Fe	Ni	Nb	Mo
Precipitation	25,99	0,17		2,33	9,89	1,65	21,19	38,79	
Matrix		0,60	0,65		26,83	5,13	62,77		4,02

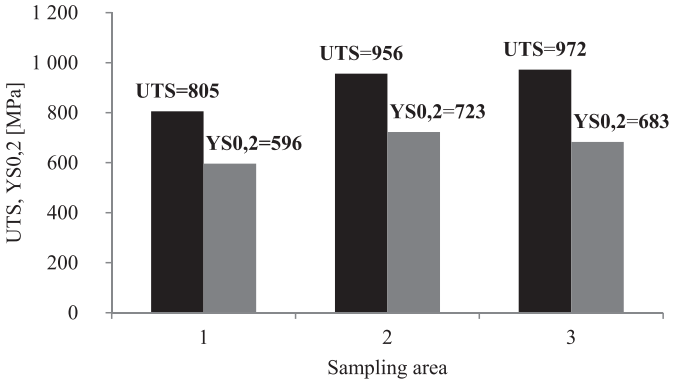

Fig.11. The results of tensile properties of the Inconel®718 sheet samples from three areas of the product (fig. 2) obtained after rotary forming with laser heating

Tensile properties of the material after deformation depends on the sampling area. Tensile strength reaches the highest value for the sample taken from the flange of the product (area 3) and it is UTS=972MPa. For the sample from the conical part of the product (area 2) it is UTS=956MPa, and the lowest value reaches for the sample taken from a cylindrical part of the product (area 1) and it is UTS=805MPa. The yield strength reaches the highest value for the sample taken from the conical part of the product (area 2) and it is $YS_{0,2}$ = 723MPa. The yield strength for the sample taken from the flange of the product (area 3) it is $YS_{0,2}$=683MPa, whereas the sample taken from the cylindrical part (area 1) it is $YS_{0,2}$=596MPa. The results show that regardless of the sampling area, the strength properties are larger than properties of the sheet in initial state. This is due to the large plastic deformation, particularly in the areas 2 and 3.

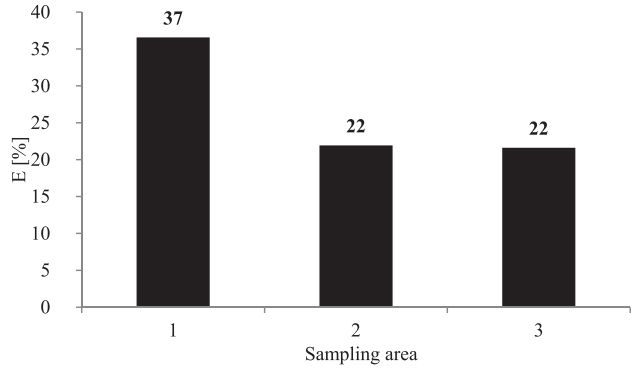

Fig.12. The results of plastic properties of the Inconel®718 material samples from three areas of the product (fig. 2) obtained after rotary forming with laser heating

Plasticity rated by elongation A, depend on the sampling area for testing. Elongation of the sample taken from the cylindrical part of the product (area 1) has the highest value E=37%. Elongation for both the sample from the conical part of the product (area 2), as well as from the flange (area 3) is E=22%. The results show a decrease in plastic properties in relation to the sheet in initial state, due to plastic deformation, especially in areas 2 and 3.

The average results of the HRC hardness carried out on samples cut out of the three areas of the finished product (fig. 2a) are shown in fig. 13.

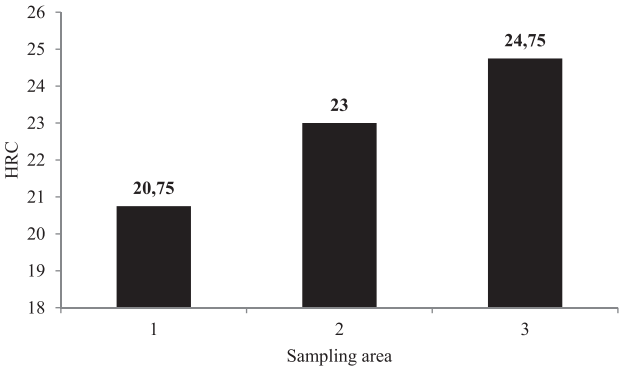

Fig.13. The results of the HRC hardness of the Inconel®718 sheet samples from three areas of the product (fig. 2) obtained after rotary forming with laser heating

HRC hardness for material taken from the area 1 has the lowest value 20,75HRC. The result is an effect that the material obtained from the upper cylindrical part is the least deformed, and thus the least strengthened. The intermediate value of hardness 23HRC is obtained from the material taken from an area 2. The highest hardness of the material 24,75HRC has an area 3.

3.2.2 The results of microstructural observations

Fig. 14 shows the structure of the Inconel®718 sheet after the rotary forming process with the laser heating, observed on a sample taken from an area 1 (fig. 2).

a) b)

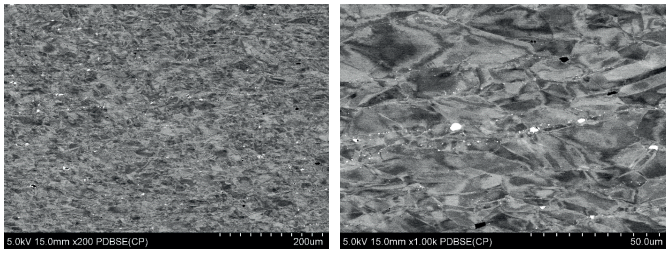

Fig.14. The structure of the Inconel®718 sheet after rotary forming process with the laser heating samples from area 1
a) ×200,
b) ×1,00k

The structure of the material is characterized by elongated grains with unclear borders. The material is not recrystallized. At the grain boundaries are small, regular precipitation, separated by larger precipitates. They are most likely the result of intensive impact of temperature during laser heating.

Fig. 15 shows the surface layer structure of the Inconel®718 sheet, on a sample taken from the area 2 (fig. 2), after the rotary forming process with laser heating.

a) b)

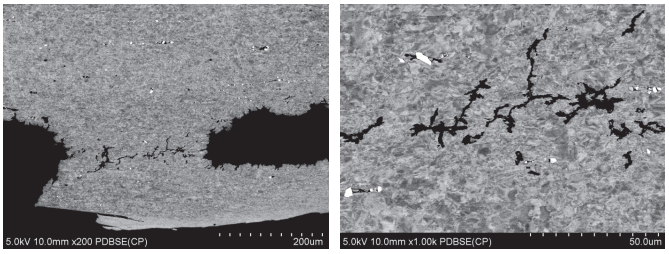

Fig. 15. The structure of the surface layer of the Inconel®718 sheet after rotary forming process with the laser heating samples from area 2
a) ×200,
b) ×1,00k

Fig. 15 shows the structure of the material separated by the deformation and rolled back to the surface. As a consequence of forming with the laser heating the material of the roll is welded with the ground (metal sheet), as illustrated in the fig. 15 (primary grain boundaries).

Fig. 16 shows the results of EDS mapping from the material shown in fig. 15a.

The consequence of the material picking off is microcracks on the surface that propagate into the material. EDS mapping confirmed the initial observations that chemical composition of the rolled layers on the surface is widely varied. Figs. 16b-c shows that the largest share in the chemical composition of the alloy are nickel and chromium, forming Inconel®718 matrix. Dark areas in fig. 16a is rich in chromium (fig. 16c) and oxygen (fig. 16e), which suggests that the areas are rich in chromium oxide phase. The dark material layers (fig. 16a) is also increased the intensity of aluminum occurrence (fig. 16h) and titanium (fig. 16i). Other elements separated on EDS analyzes, namely iron (fig. 16d), silicon (fig. 16f), molybdenum (fig. 16g) are distributed relatively evenly in the structure of rolled surface layers.

Fig. 17 shows the intensity of particular elements in the fragment of Inconel®718 from area shown in fig. 15a.

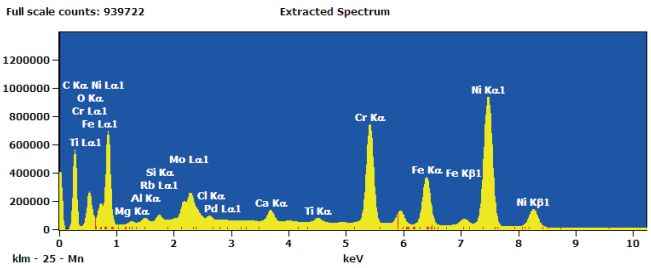

Fig.17. EDS mapping spectrum of the surface layer structure Inconel®718 sheet of area shown in fig. 14a, obtained after rotary forming process with the laser heating

On the basis of the peaks was found that the largest share in the structure of the test material are nickel, chromium, which are the matrix. Peaks of carbon are a result of the spectrum of the resin, which was SEM sample included.

Fig. 18 shows the structure of the Inconel®718, observed on a sample taken from the area 3 in (fig. 2), after rotary forming process with the laser heating.

a) b)

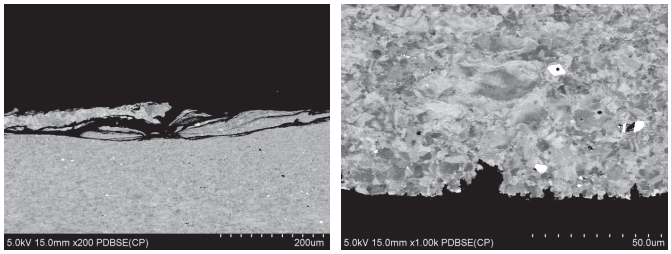

Fig. 18. The structure of surface layer structure Inconel®718 sheet cut from area 3 of the product (fig. 2) obtained after rotary forming process with the laser heating
a) ×200,
b) ×1,00k

It can be seen that the material under the high-pressure of forming roll and high temperature is peeling and rolled on the surface. The generated temperature of the laser beam is so high that the material is partially recrystallized. In fig. 18b are also visible intergranular cracks extending along the grain boundaries.

Fig. 19 shows the structure of the Inconel®718 surface, observed on a sample taken from the area 3 (fig. 2), after rotary forming process with the laser heating.

a) b)

c) d)

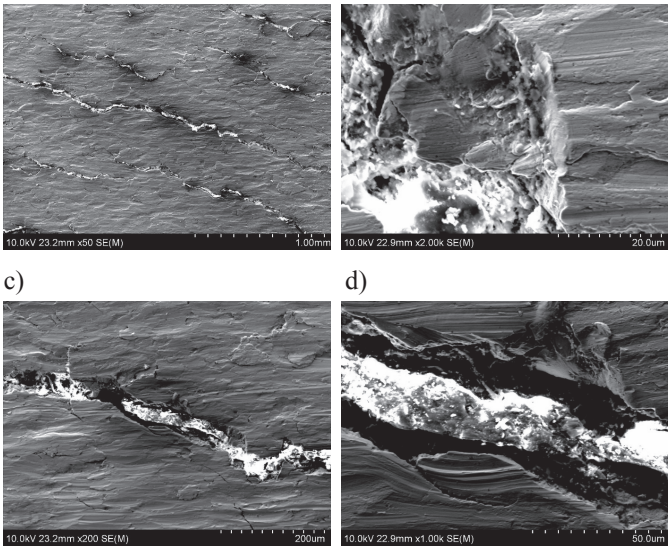

Fig. 19. The surface structure of the Inconel®718 sheet cut from a area 3 of the product (fig. 2) obtained after rotary forming process with the laser heating with visible microcracks

On the surface of the material (fig. 19) is visible dense mesh of microcracks. Cracks are distributed parallel to the direction of forming roll (fig. 19a). The brittle nature of the crack is particularly noticeable in fig. 19b. In the recesses of cracking (fig. 19c), the material is accumulated, which is due to peeling of the surface layer of formed material and rewelding on the sheet surface. On the surface of the formed material, forms a kind of layer which includes a large amount of oxides. The reason is the high temperature of the laser beam and the large unit pressure of forming roll.

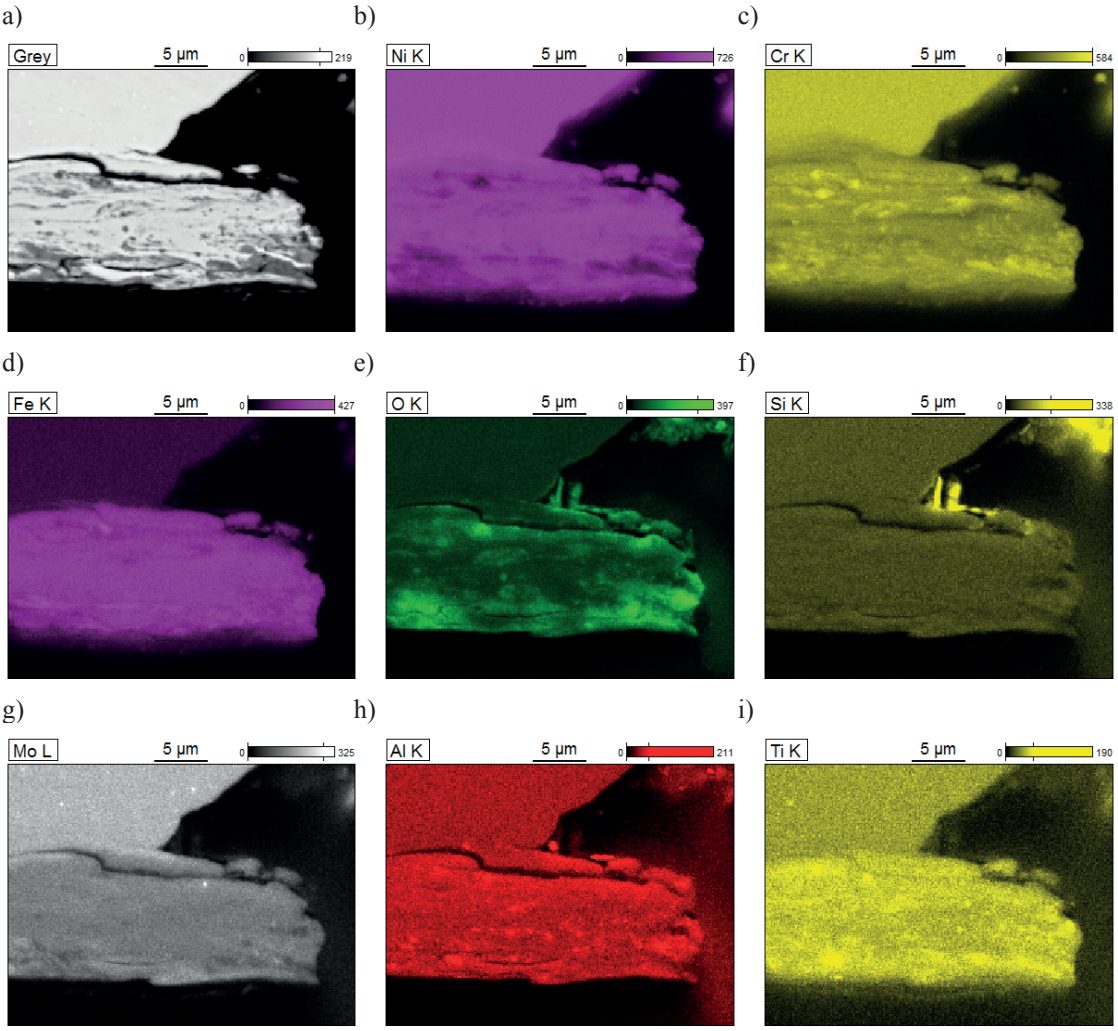

Fig. 16. The results of EDS mapping structure of the Inconel®718 surface layer of the area shown in Fig. 14a, obtained after rotary forming process with the laser heating, a) SEM image, b) the intensity distribution of nickel, c) the intensity distribution of chromium d) the intensity distribution of the iron, e) the intensity distribution of oxygen, f) of the intensity distribution of silicon, g) the intensity distribution of molybdenum, h) of the intensity distribution of the aluminum, i) of the intensity distribution of titanium

4. Conclusions

In the paper were made studies of mechanical properties and microstructure observation of the material Inconel®718 in initial state and after rotary forming process with laser heating.

Based on the results the following conclusions can be formulate:

- the results of strength and plastic properties indicate the absence of planar anisotropy of the Inconel®718 sheet in initial state,
- noteworthy preferably low value $YS_{0,2}$/UTS, regardless of the sampling direction, providing a high "store strength" of the material,
- rotary forming process, despite the laser heating, intensively affects to increase the strength properties of the material throughout the volume of the product, relative to the material in initial state. The smallest increase occurs in the flange part, increases for the conical part and reaches the highest value for the cylindrical part,
- sheet as its delivered is characterized by a recrystallized structure with clear grain boundaries,
- the structure of the material after rotary forming process with laser heating is characterized by elongated grains with amorphous grain boundaries. At the grain boundaries are small, regular precipitation of chromium, niobium, titanium and molybdenum carbides, separated by larger brittle precipitates,
- in the surface layer appear local defects in the form of peeled material and rolled on the surface, which leads to the formation of a dense grid of microcracks on the surface, which propagate into the material,
- in areas exposed on the most intense laser heating can be seen locally melted material.

Acknowledgments

Financial support of the National Center for Research and Development in the Horizontal Programme – Applied Research Programme – Project PBS1/B6/4/2012-FLOWFO is gratefully acknowledged.

REFERENCES

[1] C.T. Sims, N.S. Stoloff, W.C. Hagel, Superalloys II, Ed. J. Willey & Sons, New York 1987.

[2] C.T. Sims, A history of superalloy metallurgy for superalloy metallurgists, General Electric Company Schenectady, New York 1984.

[3] D.A. Metzler, A Gleeble® – base method for ranking the strain-age cracking susceptibility of Ni-based superalloys, Welding Journal **87**, 249-256 (2008).

[4] B.E.P. Beeston, L.K. France, The stacking fault energies of some binary nickel alloys fundamental to the Nimonic series, J. Inst. Metals **96**, 105-107 (1968).

[5] Z. Huda, T. Zaharinie, I.H.S.C. Metselaar, S. Ibrahim, J. Min Goh, Kinetics of grain growth in 718 Ni-base superalloy, Archives of Metallurgy and Materials **3**, 59, 847-852 (2014).

[6] S. Kalpakcioglu, On the mechanics of shear spinning, Journal of Engineering for Industry 83, 125-130 (1961).

[7] W. Qiang, T. Tao, Z.R. Wang, A study of the working force in conventional spinning, Proceedings of the Second International Conference on Technology of Plasticity, Springer, Berlin 1987.

[8] M. Runge, Spinning and flow forming, Leifeld GmbH Werkzeugmaschinenbau/Verlag Moderne Industrie AG, D-86895, Landsberg/Lech, 1994.

[9] C.L. Packham, Metal spinning and shear and flow forming, Sheet Metal Industries, 326-329 (1997).

[10] E. Quigley, J. Monaghan, Metal forming: an analysis of spinning proces, Journal of Materials Processing Technology **103**, 114-119 (2000).

[11] C.C. Wong, T.A. Dean, J. Lin, A review of spinning, shear forming and flow forming processes, International Journal of Machine Tools & Manufacture, 43, 1419-1435 (2003).

[12] A. Plewiński, T. Dregner, Spinning and flow forming hard-to-deform metal alloys, Archives of Civil and Mechanical Engineering **9**, 1, 101-109 (2009).

[13] M. Nowosielski, K. Żaba, M. Kwiatkowski, D. Woźniak, T. Pieja, Influence of rotary forming process parameters on the quality of the final products made of nickel superalloys (Inconel®) sheets, ICNFM 2014, Wisła, Poland, June 4–6 2014, book of abstracts.

[14] M. Kwiatkowski, K. Żaba, M. Nowosielski, D. Pociecha, T. Tokarski, P. Kita, Temperature measurement in the rotary forming process of a nickel superalloys (INCONEL) sheet during induction heating, Key Engineering Materials **622-623**, 823–830 (2014).

[15] ISO 6892-1:2009, „Metallic materials – Tensile testing – Part 1: Method of test at room temperaturę".

[16] ISO 6508-1:2005, „Metallic materials – Rockwell hardness test – Part 1: Test method (scales A, B, C, D, E, F, G, H, K, N, T)".

[17] G. Vander Voort, Metallography of superalloys, Industrial Heating **70**, 40-43 (2003).

[18] G. Appa Rao, K. Satya Prasad, M. Kumar, M. Srinivas, D.S. Sarma, Effect of standard heat treatment on the microstructure and mechanical properties of hot isostatically pressed superalloy inconel 718, J. Mater. Sci. Technol. **19**, 1-9 (2003).

Received: 10 January 2015.